Title

Non-local dielectric effects in nanoscience

Journal

The Journal of Chemical Physics, 159(2)

ISSN

0021-9606

Authors

Raja, Archana

Brus, Louis E

Publication Date

2023-07-14

DOI

10.1063/5.0150293

Peer reviewed

The Journal of Chemical Physics

RESEARCH ARTICLE | JULY 14 2023

Non-local dielectric effects in nanoscience

Special Collection: 40 Years of Colloidal Nanocrystals in JCP

Archana Raja ; Louis E. Brus

J. Chem. Phys. 159, 020901 (2023)
https://doi.org/10.1063/5.0150293

The Journal of Chemical Physics PERSPECTIVE pubs.aip.org/aip/jcp

Non-local dielectric effects in nanoscience

Cite as: J. Chem. Phys. 159, 020901 (2023); doi: 10.1063/5.0150293
Submitted: 13 March 2023 • Accepted: 19 June 2023 •
Published Online: 14 July 2023

Archana Raja[1,a] and Louis E. Brus[2]

AFFILIATIONS

[1] Molecular Foundry, Lawrence Berkeley National Laboratory, Berkeley, California 94720, USA
[2] Department of Chemistry, Columbia University, New York, New York 10027, USA

Note: This paper is part of the JCP Special Topic on 40 Years of Colloidal Nanocrystals in JCP.
[a] **Author to whom correspondence should be addressed:** araja@lbl.gov

ABSTRACT

The physical properties of charges and excitations in nanoscale materials are influenced both by the dielectric properties of the material itself and the surrounding environment. This non-local dielectric effect was first discussed in the context of molecules in solvents over a century ago. In this perspective, we discuss non-local dielectric effects in zero-dimensional, one-dimensional, and two-dimensional nanoscale systems.

INTRODUCTION

For a century, chemists have understood the importance of the solvent dielectric constant. Salts dissolve into ions in water but not in hydrocarbon solvents because a higher dielectric constant stabilizes ionic species. The Coulomb force between two ions is reduced ("screened") by electric-field-induced polarization in solvent molecules. At higher ion concentrations, the force is reduced further by dynamic screening, where one ion attracts a cloud of oppositely charged ions. Debye's analysis of this effect, introducing the concept of screening length, is a milestone of early theoretical chemistry.[1] Debye screening also occurs at charged interfaces in electrochemical cells and solid-state devices.

In the Marcus model for electron transfer kinetics, the key feature is solvent dielectric polarization by electric fields from solute electric dipoles and/or charge.[2] When an electron transfers, the change in the polarization ("reorganization energy") determines the rate. There is both an inner reorganization energy due to a change in the solute structure and an outer energy due to the solvent. The outer energy is treated by continuum dielectric theory and dominates in high dielectric constant environments. In kinetic processes, the time scale of dielectric response is important. The reorganization energy comes from the "slow" response, such as solvent dipole rotation and/or solute structural change, and not from the "fast" response of electronic polarization. Warshel[3] recognized the necessity of including solvation energies in quantum mechanical calculations of biological enzyme catalysis. He built explicit models of protein dipoles stabilizing substrates in ionic transition states. In both Marcus and Warshel models, solvation determines the kinetics of a chemical reaction. In inorganic nanoscience, dielectric constants are often larger than in proteins and organic solutions, and thus, solvation effects should be strong.

The regions of quite different dielectric constants are often intimately connected in nanoscale systems. Even though a charge or excited state is located in one region, its stability, screening, and dynamics are influenced by the dielectric constants of all nearby regions. This is the "non-local" dielectric effect. Such effects are strongly geometry-dependent and are important both at low frequencies in electrostatic problems and at high frequencies (THz to visible) in spectroscopic problems. In this tutorial review, we outline some experimental consequences of non-local effects, with examples taken mostly from our research. Note there is also a recent perspective on non-locality involving metal particles and surfaces.[4]

QUANTUM DOTS

Quantum dots (Qdots) of several nm size have hundreds or thousands of atoms. Along short Qdot dimensions, individual electrons and holes can show quantized motion.[5] Yet much of Qdot science can be captured by continuum dielectric ideas that coarse grain over actual structure. This approximation is used throughout inorganic nanoscience. The simplest Qdot model is a round neutral polarizable sphere. If such a Qdot with a higher dielectric constant than the surroundings contains an extra electron or hole, there is a polarizability force pulling this charge to the center, away from the surface.[6] The electric field lines of the internal charge cross the Qdot surface into the solvent and terminate at infinity—in this way,

the charge senses the outside dielectric constant. This implies that a single electron or hole is relatively more stable in a larger Qdot. The ionization potential, electron affinity, and redox potential are size-dependent for purely electrostatic reasons, in addition to any size dependence related to quantum size effects in the band structure. If the particle dielectric constant goes to infinity in a model metallic particle in vacuum, then the ionization energy increases by $1/2\ e^2/a$ over the bulk work function, and the electron affinity decreases by this same amount.[7] Here, e is the electron charge, and a is the particle radius. Many deeper-level calculations have been done on explicit Qdot structures, such as wurtzite CdSe nanocrystals with a permanent dipole moment in a polarizable external medium.[8]

Qdots on surfaces can focus and magnify electric fields. Neutral 12 nm PbSe Qdots are highly polarizable with a static dielectric constant of about 200.[9] If deposited on a Si substrate with a 1.2 nm surface oxide, occasionally a Qdot will sit directly over a static charge in the oxide. The Qdot almost completely screens the charge Coulomb field from its interior, developing a strongly induced dipole. This dipole creates a static electric field "hotspot" directly above the Qdot, where the Coulomb field is stronger than it would be without the Qdot.[10]

A Qdot excited electronic state ("exciton") can be modeled as a neutral polarizable sphere containing both an electron and a hole. Here, the electric field lines begin on the hole and terminate on the electron. To the extent that the lines fringe outside the Qdot, the Coulomb attraction between the electron and hole is stronger (less screened) in the Qdot than in the bulk semiconductor. The attraction depends on the exact locations of the electron and hole, as well as their separation. Because the electron and hole are close together in one Qdot, and the Coulomb force is less screened, the exciton binding energy can be an order of magnitude stronger than in the 3D bulk crystal. The change in the local screening due to the exterior solvent also causes renormalization of Qdot exciton energy levels, leading to changes in the bandgap, electron affinity, and ionization potential, similar to a molecule on a surface.[11]

An exterior medium can also affect Qdot kinetics, as in the Marcus theory. Si Qdot emission in porous silicon films is strong with vacuum in the local pores but absent for pores containing water. As the intrinsic Si internal reorganization energy is small, this appears to be a case where kinetics is dominated by the external reorganization energy.[12]

The large size of Qdots compared to molecules causes the Rayleigh scattering to be significant at optical frequencies. Figure 1 is the well-known figure of screening of an incident electromagnetic wave $\boldsymbol{E}_{inc}$ by a round particle in vacuum, creating a total oscillating polarization $\boldsymbol{P}$ of the Qdot as a whole,

$$\boldsymbol{P} = 4\pi\left(\frac{\epsilon - 1}{\epsilon + 2}\right)a^3\boldsymbol{E}_{inc}.$$

$\boldsymbol{P}$ is a **coherent** response, in that the particle electronic polarization is fast enough to track the rise and fall of the incoming electromagnetic wave with definite amplitude and phase. $\boldsymbol{P}$ is a local mode of the electromagnetic field induced by the dielectric response of the particle. The oscillating $\boldsymbol{P}$ can emit (scatter) light, analogous to the light emitted by an excited state transition dipole of a molecule. In both cases, the emission rate is proportional to the $\boldsymbol{P}^2$ (absolute magnitude). Thus, the emission rate (scattering rate) is proportional to the square of the particle volume ($\sim a^3$), i.e., the number of atoms to the sixth power. This is the signature of a coherent process.

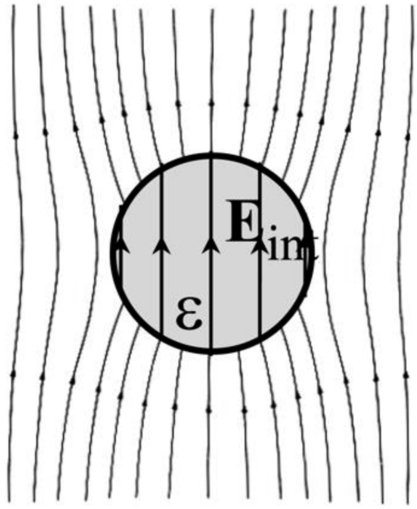

FIG. 1. Screening inside a particle with dielectric function ε in vacuum due to an incident electric field.

The coherent oscillating electric field of $\boldsymbol{P}$ can add constructively or destructively to the incident plane wave. This creates nearby regions of light intensity either greater ("hot") or less than that of the incident plane wave. A molecule in a hotspot will show increased Raman scattering—this is the surface-enhanced Raman (SERS) effect. The effect is "doubled" in a sense, in that the molecule initially sees a more intense laser field. The irradiated molecule creates a Raman oscillating dipole, red-shifted from the laser frequency. In turn, the molecular Raman dipole induces an image Raman dipole in the nearby particle. The combined Raman dipoles emit Raman light faster than would occur from the molecular Raman dipole alone.

The particle scattering pattern, induced by the surface dielectric discontinuity, is exquisitely sensitive to the local environment. If a second particle is located some distance above the north pole of the first, then the lower particle sees both the incident field and the local field of the upper particle oscillating dipole. The polarization density inside the lower particle increases and, instead of being uniform across the particle, becomes more localized on the surface near the north pole. An analogous process occurs in the upper particle. This coherent interaction causes the hotspot in the junction between the particles to become more intense. For large Ag particles, a nanometer or so apart, the field can increase by orders of magnitude, becoming so intense as to enable the detection of single-molecule Raman scattering in the junction.[14–16] Molecular photochemistry can also be enhanced near particles under specific circumstances.[17] Figure 2 is an illustration of such a hotspot between three particles.

There is also an optically induced dipole–dipole attraction between particles, scaling with the intensity of the irradiating field.[18] In the dark without irradiation, the van der Waals attraction between

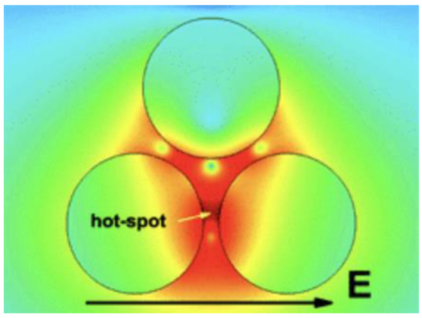

FIG. 2. Enhancement of electric field between metal nanoparticles: as the distance between the particles approaches a nanometer, the electric field between the particles increases by many orders of magnitude in response to an external E, as indicated by the intense red hotspot between the particles.[13] Etchegoin *et al.*, Phys. Chem. Chem. Phys. 8, 1463–9076 (2006); licensed under a Creative Commons Attribution (CC BY) license.

particles is due to the correlated electromagnetic attraction of instantaneous quantum dipole fluctuations at all frequencies across the spectrum.[19] Both the van der Waals attraction and the attraction in a light field can be screened by the fast electronic response of the nearby solvent.[20] For example, screening is critical when a solution of Qdots in hexane is dried on a graphite surface. The initial dilute solution behaves as a Qdot gas. Upon drying, the hexane evaporates, and the van der Waals interaction between Qdots increases by a factor of about 4, causing a 2D gas-liquid phase transition to liquid droplets composed solely of Qdots on the flat surface.[21,22]

A substrate also substantially modifies luminescence, as well as causing the renormalization of exciton energy levels. For example, on a glass coverslip, most of the luminescence goes into evanescent waves propagating along the surface rather than into perpendicular plane wave emission into free space.[23] Screening of the emitted wave in the higher index cover slip causes the purely radiative lifetime to be about a factor of 3 longer for transition dipoles perpendicular to the surface compared with those parallel to the surface.

If the substrate can also absorb luminescence, then there is an interesting interplay between near-field energy transfer and screening. Both graphite and MoS_2 are easily exfoliated van der Waals solids. With each, it is possible to prepare thin flat substrates of just several or even a single monolayer. In these absorbing materials, the real part of the dielectric constant can screen Qdot emission (analogous to the glass coverslip), while the imaginary part opens the possibility of energy transfer into the substrate, analogous to Förster energy transfer of molecules in solution. Graphite and MoS_2 show differing screening and energy transfer behavior.[24,25] Excited state Qdot energy transfer increases with the increasing substrate thickness for graphite but decreases with thickness in MoS_2. This occurs because screening is significantly weaker in graphite than in MoS_2 at the optical frequency of the Qdot emission. In MoS_2, enhanced screening (growing as the square of the substrate volume) from multiple layers increasingly prevents emission field penetration into the substrate, thus decreasing the energy transfer. In contrast, in few-layer graphene substrates, all layers accept energy as the emission field is not strongly screened and, thus, penetrates deeper. Note that few-layer graphenes also show an intrinsic Raman G peak that increases with the thickness due to weak screening of the incident laser.[26] Bulk graphite appears black and not shiny to the eye because screening is weak.

2D AND 1D NANOSYSTEMS

Single-layer transition metal dichalcogenides, such as MoS_2, are 2D semiconductors in which electrons and holes are mobile in the plane. As electrons and holes separate, a greater fraction of their attractive Coulomb electric field fringes out of the monolayer. For a monolayer in vacuum, at short separations, the Coulomb interaction is partially screened, varying as $\log(r^{-1})$, where r is the electron–hole separation.[27,28] At distances that are large with respect to the monolayer thickness, the Coulomb interaction is almost unscreened. The electron and hole form a series of excited states or Rydberg states as they separate, extrapolating ultimately to the continuum quasiparticle bandgap energy. The Rydberg pattern energies deviate from the theoretical 2D hydrogen atom model as screening decreases with increasing exciton diameter. The 2D exciton binding energy is large because screening is weak compared with 3D semiconductors. In monolayer WS_2 supported on fused silica, the lowest 1s exciton binding energy is 0.32 eV with an extrapolated bandgap of 2.33 eV.[29–34] More generally, the binding energies of such monolayer systems are hundreds of meV. Note that other clear examples of this effect are given by "dielectric confinement" in bulk layered perovskites and Qdot platelets.[35–38]

In 3D bulk semiconductors, the bandgap is an intrinsic property. In contrast, the above discussion shows that the bandgap of a 2D monolayer semiconductor depends upon the local environment. The increased nearby screening will decrease exciton binding energies and, thus, the extrapolated bandgap, leaving the exciton energy itself nearly unchanged. This effect was demonstrated when a small patch of graphene bilayer was deposited on a larger WS_2 monolayer. Under the graphene, the WS_2 bandgap was 2.20 eV, 0.135 eV smaller than in areas without graphene (Fig. 3).[39] The area under graphene is essentially a potential well for free carriers. A detailed calculation indicates that WS_2 directly under the graphene edges forms an in-plane heterostructure. The change in the local dielectric environment causes a rigid shift of the valence and conduction bands, with the band structure of the WS_2 being preserved,[40] analogous to the screening of molecular electronic levels on surfaces. One might imagine that systematic patterning of dielectric overlayers on 2D monolayers opens the possibility of creating complex structures and devices. An example of this was recently demonstrated.[41] Also, in systems where phonon energies are on the same order of magnitude as the exciton binding energy, the two can significantly interact.[42] The frequency dependence of the dielectric screening can also be used to tune the binding energies and bandgaps. For instance, with increasing charge-carrier density, there is an enhanced screening at the plasma frequency.[43]

Semiconductor Single Wall Carbon Nanotubes (SWNTs) of 1 nm diameter are close to being 1D systems. As such, their excitons are sensitive to screening by surrounding solvent in an analogous fashion to 2D monolayers discussed above. With low external screening, exciton effects are so strong as to completely dominate optical absorption and luminescence.[44,45] The binding energy of the

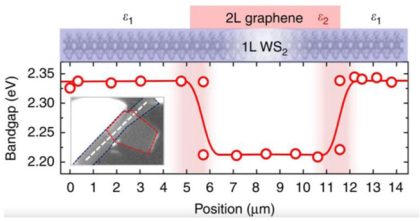

FIG. 3. Coulomb engineering of the bandgap in 2D materials. Spatially dependent bandgap energy extracted from the exciton peak positions along the profile of the lateral WS2/graphene heterostructure, as illustrated in the schematic representation and marked by the dashed line in the inset optical micrograph.[34] Raja *et al.*, Nat. Commun. **8**, 15251 (2017); licensed under a Creative Commons Attribution (CC BY) license.

lowest exciton in the (6,5) tube is 0.42 eV, about one-third of the bandgap energy itself.

In SWNT, the pi electrons and holes are right on the surface, and the sensitivity to external screening is strong. In contrast, in semiconductor Qdots, the quantum-confined electron and hole wavefunctions derive from interior band states with nodes on the surface. External screening is less important.

SWNTs also provide another example of coherent optical scattering. As discussed above, in an approximate sense, optical (Rayleigh) scattering grows as the square of the volume, while exciton incoherent optical absorption grows linearly. Individual long SWNTs extending across a focused laser spot show significant Raleigh scattering that can be used to identify and characterize them.[45–47] This is especially important for metallic SWNTs that do not luminesce. Scattering is strong for incident light polarization along the tube length. For perpendicular polarization, scattering is weak as the SWNT itself screens the incident field.

FINAL REMARKS

Just as in other areas of chemistry, the local dielectric environment has a profound impact on nanoscale systems. Nanoscience properties, in a sense, are hybrid between those of molecules and the bulk solid-state. The fundamental concepts of how electronic states and charge carriers are influenced by neighboring dielectric, magnetic, or even multiferroic environments could open opportunities for new devices. Applications may occur in microelectronics, especially with scaling of feature sizes for control of the flow of energy, charge, and spin, as well as in quantum information science where the local environment is key to controlling decoherence processes. Progress in this direction critically depends on further advances in nanofabrication and chemical synthesis.

ACKNOWLEDGMENTS

A.R. was supported by the Office of Science, Office of Basic Energy Sciences, U.S. Department of Energy, under Contract No. DE-AC02-05CH11231. We thank the reviewers for their insightful comments.

AUTHOR DECLARATIONS

Conflict of Interest

The authors have no conflicts to disclose.

Author Contributions

Archana Raja: Conceptualization (equal); Writing – original draft (equal); Writing – review & editing (equal). **Louis Brus**: Conceptualization (equal); Writing – original draft (equal); Writing – review & editing (equal).

DATA AVAILABILITY

Data sharing is not applicable to this article as no new data were created or analyzed in this study.

REFERENCES

[1] P. Debye and E. Hückel, Phys. Z. **24**, 185 (1923).
[2] R. A. Marcus, J. Chem. Phys. **24**, 979 (1956).
[3] A. Warshel, Acc. Chem. Res. **14**, 284 (1981).
[4] V. N. Peters, S. Prayakarao, S. R. Koutsares, C. E. Bonner, and M. A. Noginov, ACS Photonics **6**, 3039 (2019).
[5] A. L. Efros and L. E. Brus, ACS Nano **15**, 6192 (2021).
[6] L. E. Brus, J. Chem. Phys. **79**, 5566 (1983).
[7] G. Makov, A. Nitzan, and L. E. Brus, J. Chem. Phys. **88**, 5076 (1988).
[8] E. Rabani, B. Hetényi, B. J. Berne, and L. E. Brus, J. Chem. Phys. **110**, 5355 (1999).
[9] H. Bilz, A. Bussmann-Holder, W. Jantsch, and P. Vogl *Dynamical Properties of IV–VI Compounds* (Springer, 2006).
[10] C. H. Ben-Porat, O. Cherniavskaya, L. Brus, K.-S. Cho, and C. B. Murray, J. Phys. Chem. A **108**, 7814 (2004).
[11] J. B. Neaton, M. S. Hybertsen, and S. G. Louie, Phys. Rev. Lett. **97**, 216405 (2006).
[12] L. Brus, Phys. Rev. B **53**, 4649 (1996).
[13] P. G. Etchegoin, C. Galloway, and E. C. Le Ru, Phys. Chem. Chem. Phys. **8**, 2624 (2006).
[14] J. Jiang, K. Bosnick, M. Maillard, and L. Brus, J. Phys. Chem. B **107**, 9964 (2003).
[15] M. Inoue and K. Ohtaka, J. Phys. Soc. Jpn. **52**, 3853 (1983).
[16] A. M. Michaels, Jiang, and L. Brus, J. Phys. Chem. B **104**, 11965 (2000).
[17] A. Nitzan and L. E. Brus, J. Chem. Phys. **75**, 2205 (1981).
[18] P. L. Redmond, A. J. Hallock, and L. E. Brus, Nano Lett. **5**, 131 (2005).
[19] E. M. Lifshitz, J. Exp. Theor. Phys. USSR **29**, 94 (1955).
[20] H. C. Hamaker, Physica **4**, 1058 (1937).
[21] G. Ge and L. Brus, J. Phys. Chem. B **104**, 9573 (2000).
[22] E. Rabani, D. R. Reichman, P. L. Geissler, and L. E. Brus, Nature **426**, 271 (2003).
[23] W. Lukosz and R. E. Kunz, J. Opt. Soc. Am. **67**, 1607 (1977).
[24] A. Raja, A. Montoya–Castillo, J. Zultak, X.-X. Zhang, Z. Ye, C. Roquelet, D. A. Chenet, A. M. van der Zande, P. Huang, S. Jockusch, J. Hone, D. R. Reichman, L. E. Brus, and T. F. Heinz, Nano Lett. **16**, 2328 (2016).
[25] F. Prins, A. J. Goodman, and W. A. Tisdale, Nano Lett. **15**, 3655 (2015).
[26] N. Jung, A. C. Crowther, N. Kim, P. Kim, and L. Brus, ACS Nano **4**, 7005 (2010).
[27] N. S. Rytova, in *Proceeding of the MSU, Phys., Astron.* (Springer, 1967), Vol. 3.
[28] L. V. Keldysh, Sov. J. Exp. Theor. Phys. Lett. **29**, 658 (1979).
[29] K. He, N. Kumar, L. Zhao, Z. Wang, K. F. Mak, H. Zhao, and J. Shan, Phys. Rev. Lett. **113**, 026803 (2014).
[30] A. Chernikov, T. C. Berkelbach, H. M. Hill, A. Rigosi, Y. Li, O. B. Aslan, D. R. Reichman, M. S. Hybertsen, and T. F. Heinz, Phys. Rev. Lett. **113**, 076802 (2014).
[31] H. M. Hill, A. F. Rigosi, C. Roquelet, A. Chernikov, T. C. Berkelbach, D. R. Reichman, M. S. Hybertsen, L. E. Brus, and T. F. Heinz, Nano Lett. **15**, 2992 (2015).

[32]M. M. Ugeda, A. J. Bradley, S.-F. Shi, F. H. da Jornada, Y. Zhang, D. Y. Qiu, W. Ruan, S.-K. Mo, Z. Hussain, Z.-X. Shen, F. Wang, S. G. Louie, and M. F. Crommie, Nat. Mater. **13**, 1091 (2014).
[33]Z. Ye, T. Cao, K. O'Brien, H. Zhu, X. Yin, Y. Wang, S. G. Louie, and X. Zhang, Nature **513**, 214 (2014).
[34]B. Zhu, X. Chen, and X. Cui, Sci. Rep. **5**, 9218 (2015).
[35]T. Ishihara, X. Hong, J. Ding, and A. V. Nurmikko, Surf. Sci. **267**, 323 (1992).
[36]E. A. Muljarov, S. G. Tikhodeev, N. A. Gippius, and T. Ishihara, Phys. Rev. B **51**, 14370 (1995).
[37]K. Tanaka, T. Takahashi, T. Kondo, T. Umebagashi, K. Asai, and K. Ema, Phys. Rev. B **71**, 045312 (2005).
[38]B. Ji, E. Rabani, A. L. Efros, R. Vaxenburg, O. Ashkenazi, D. Azulay, U. Banin, and O. Millo, ACS Nano **14**, 8257 (2020).
[39]A. Raja, A. Chaves, J. Yu, G. Arefe, H. M. Hill, A. F. Rigosi, T. C. Berkelbach, P. Nagler, C. Schüller, T. Korn, C. Nuckolls, J. Hone, L. E. Brus, T. F. Heinz, D. R. Reichman, and A. Chernikov, Nat. Commun. **8**, 15251 (2017).
[40]L. Waldecker, A. Raja, M. Rösner, C. Steinke, A. Bostwick, R. J. Koch, C. Jozwiak, T. Taniguchi, K. Watanabe, E. Rotenberg, T. O. Wehling, and T. F. Heinz, Phys. Rev. Lett. **123**, 206403 (2019).
[41]M. I. B. Utama, H. Kleemann, W. Zhao, C. S. Ong, F. H. da Jornada, D. Y. Qiu, H. Cai, H. Li, R. Kou, S. Zhao, S. Wang, K. Watanabe, T. Taniguchi, S. Tongay, A. Zettl, S. G. Louie, and F. Wang, Nat. Electron. **2**, 60 (2019).
[42]M. R. Filip, J. B. Haber, and J. B. Neaton, Phys. Rev. Lett. **127**, 067401 (2021).
[43]R. Huber, F. Tauser, A. Brodschelm, M. Bichler, G. Abstreiter, and A. Leitenstorfer, Nature **414**, 286 (2001).
[44]F. Wang, G. Dukovic, L. E. Brus, and T. F. Heinz, Science **308**, 838 (2005).
[45]G. Dukovic, F. Wang, D. Song, M. Y. Sfeir, T. F. Heinz, and L. E. Brus, Nano Lett. **5**, 2314 (2005).
[46]M. Y. Sfeir, F. Wang, L. Huang, C.-C. Chuang, J. Hone, S. P. O'Brien, T. F. Heinz, and L. E. Brus, Science **306**, 1540 (2004).
[47]M. Y. Sfeir, T. Beetz, F. Wang, L. Huang, X. M. H. Huang, M. Huang, J. Hone, S. O'Brien, J. A. Misewich, T. F. Heinz, L. Wu, Y. Zhu, and L. E. Brus, Science **312**, 554 (2006).